U.S. DEPARTMENT OF ENERGY | Office of NUCLEAR ENERGY

Clean. Reliable. Nuclear.

3-D Chemo-Mechanical Degradation State Monitoring, Diagnostics and Prognostics of Corrosion Processes in Nuclear Power Plant Secondary Piping Structures

Advanced Sensors and Instrumentation Annual Webinar

October 29 – November 1, 2019

Douglas Adams
Vanderbilt University

Project Overview—Goals and Objectives

- Goal and Objective
  - Develop smart film to sense chemo-mechanical state of inner wall of pipe structure.
  - Utilize vibro-acoustic sensing to detect changes to inner wall of pipe due to material loss.
  - Print multi-physics transducers for power harvesting and sensing on surface of pipe.
  - Map damage inside pipe using a 3-D sensing network on outside.
  - Simulate sensing approach on a subscale cooling circuit testbed.
  - Optimize sensors and algorithms using Bayesian method.

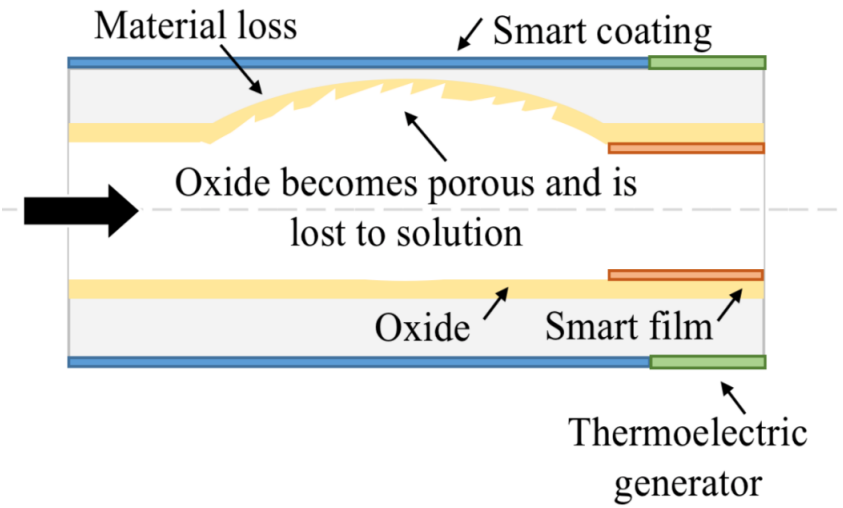

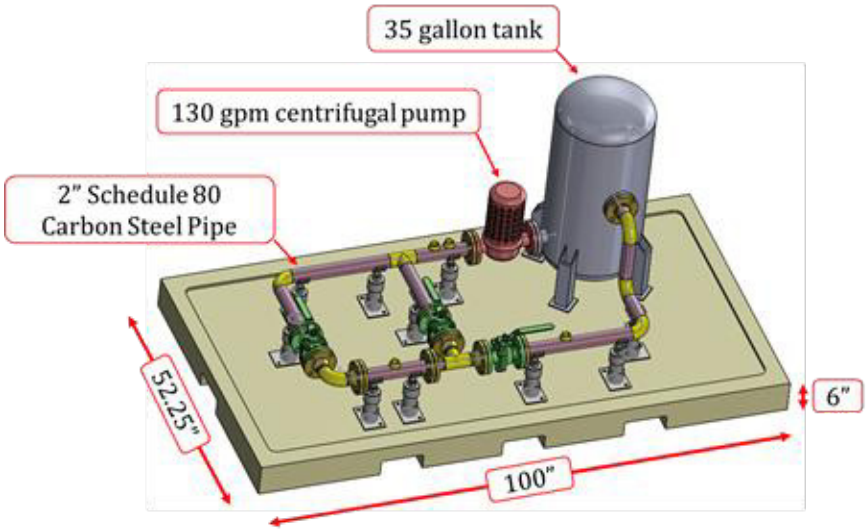

Project Overview—Participants

VANDERBILT School of Engineering

Prof. Doug Adams

Cole Brubaker

Thomas Stilson

Dave Koester

Garrett Thorne

Liudmyla Prozorovska

Prof. Kane Jennings

Xuanli (Ricky) Deng

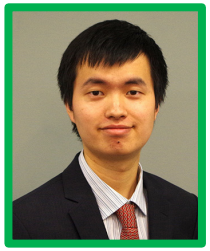

Prof. Sankaran Mahadevan

Prof. Yanliang Zhang

INL Idaho National Laboratory

Dr. Vivek Agarwal

Project Overview—Yr 2 Schedule

- Schedule
  - Year 1
    - Major Milestone: Operational cooling circuit testbed VU (Adams)
    - Minor Milestone: Thermoelectric power harvesters ND (Zhang)
    - Minor Milestone: Demonstrate smart layer VU (Jennings)
  - **Year 2**
    - **Major Milestone: Algorithms for diagnosis in pipe INL (Agarwal)**
    - **Minor Milestone: Mapping of internal surface damage VU (Adams)**
    - **Minor Milestone: Smart layer in pipe VU (Jennings)**
  - Year 3
    - Major Milestone: Prognosis and optimization of sensor network INL (Agarwal) and VU (Mahadevan)
    - Minor Milestone: Piezo network printed on component ND (Zhang)
    - Minor Milestone: Damage mapping of pipe VU (Adams)

Accomplishments – Data Collection

- Milestone: Demonstrate Diagnostic Algorithms on a Piping Structural Component
- Sampling rate 52100 samples/s
- Sampling duration: 3.2 seconds
- Data collection type:
  - Baseline, mass addition, and mass removal
- Mass addition (in grams):
  - 2.9, 6.7, 11.4, 13.8, and 23.5
- Mass removal (in grams):
  - 19, 32, 48, 63, 79, and 95
- Experimental test bed operated at 80 deg. C and pump at 60 Hz
- 10 Trails collected at each sensor location for each data collection type

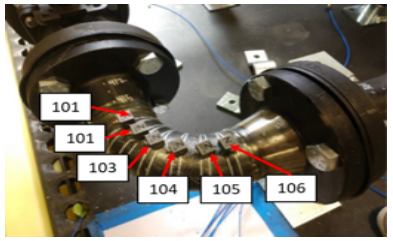

Pipe-elbow accelerometers and mass

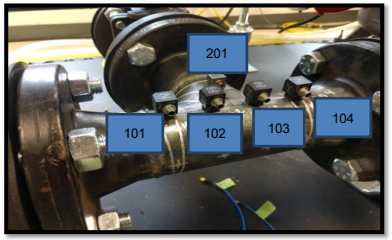

Pipe-Tee accelerometers and mass

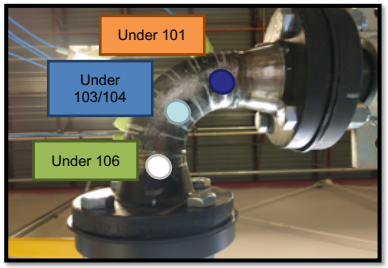

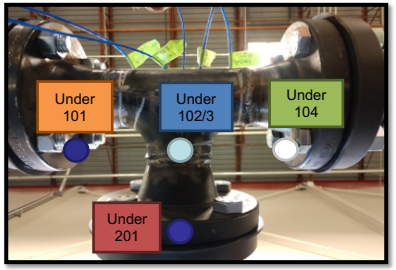

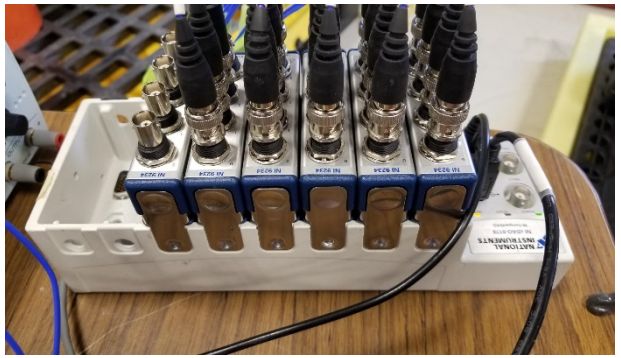

National Instruments NI cDAQ-9178 with NI 9234 data acquisition card.

Accomplishments – Diagnostic Algorithm Approach

- Vibration signal from each accelerometer is decomposed using empirical mode decomposition
- For any signal $\boldsymbol{x(t)}$, IMFs are determined using a "sifting process" as
  - Create envelope signal $c_k(t)$ with local maxima and minima
  - Get IMF_j: $\mathrm{r_j(t)} = x(t) - c_j(t)$
  - Set $x(t) = r_j(t)$ and repeat above steps until zero maxima or minima
- Seven features are extracted for each IMFs in each accelerometer directions (X, Y, and Z)
- To address of curse of dimensionality features space is reduced by feature selection
  - Permutation importance (PI)
  - Principal component analysis (PCA)

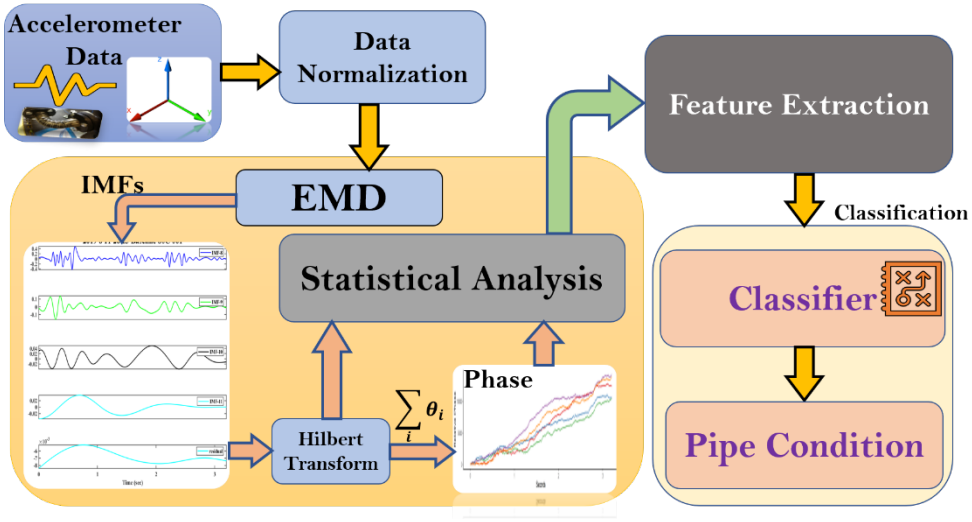

Energy (E)

$$\sum_{j=1}^{N} |X_j|^2$$

Entropy (EN)

$$-\sum_{j=1}^{N} X_j^2 \log(X_j)^2$$

Mean (μ)

$$\frac{1}{N}\sum_{j=1}^{N} X_j$$

Standard Deviation (σ)

$$\sqrt{\frac{1}{N}\sum_{j=1}^{N}(X_j - \mu)^2}$$

Skewness (SK)

$$\frac{\sum_{j=1}^{N}(X_j - \mu)^3}{\sigma^3}$$

Kurtosis

$$\frac{\sum_{j=1}^{N}(X_j - \mu)^4}{\sigma^4}$$

Slope of total phase,

$$\frac{d\theta}{dt} = \theta_t - \theta_{t-1}$$

Accomplishments – Empirical Mode Decomposition

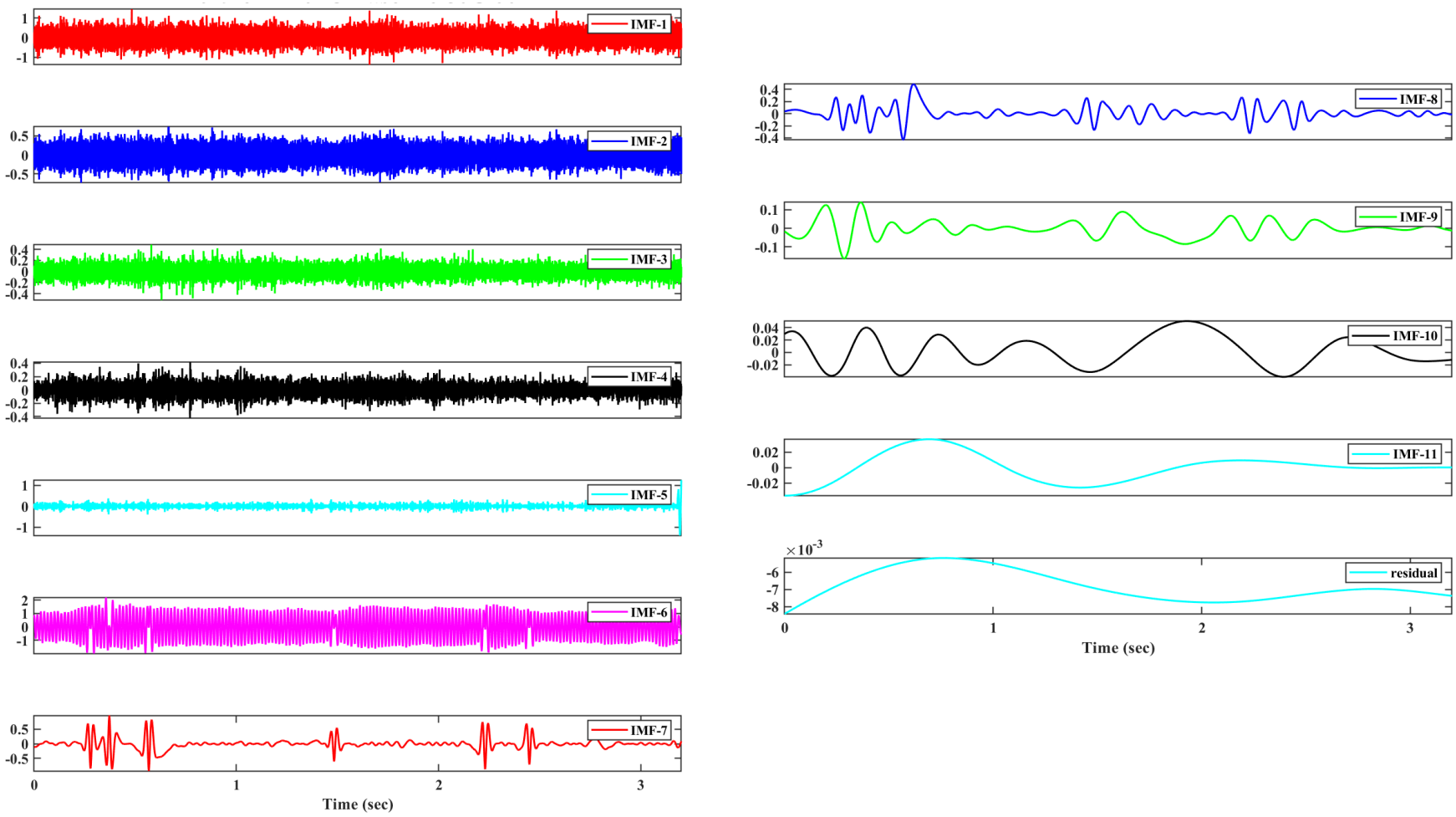

Accomplishments – Results

- Logistic Regression
  - Predict Baseline/Mass Addition using phase and time information
  - Generalized linear model for Binomial data with logit link:

$$log\left[\frac{\pi_B}{1-\pi_B}\right] = \beta_0 + \beta_1 * phase + \beta_2 * time$$

  - Model fit using Maximum Likelihood Estimation by maximizing the likelihood function iteratively using the Newton-Rhapson Method

$$L(\boldsymbol{\beta}|y) = \sum_{i=1}^{n} log\binom{n_i}{n_i y_i} + \frac{y_i * \theta - \log[1+\exp\{\theta\}]}{\frac{1}{n_i}} \text{ where } \theta = log[\frac{\pi_B}{1-\pi_B}]$$

- Classification:
  - Baseline versus Mass Addition
  - Baseline versus Mass Removal
- Machine Learning Algorithms
  - Random Forest (RF)
  - Support Vector Machines (SVM)

Random Forest

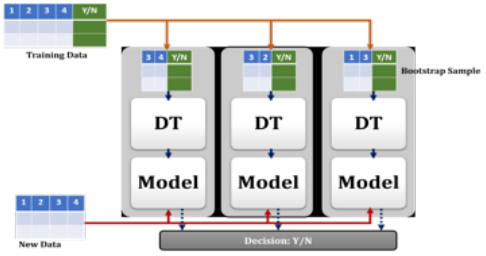

Support Vector Machines

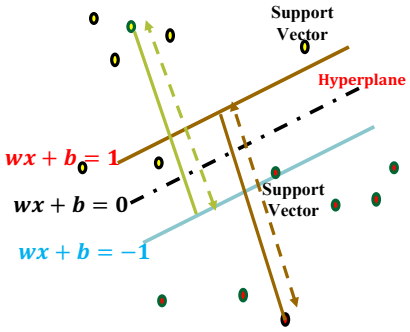

Accomplishments – Prediction Results

Classification results using random forest algorithm

Case	Training accuracy	Testing accuracy
Mass Removal (RF)	99.6%	97.3%
Mass Addition (RF)	98.8 %	95.2%

Classification results using support vector machines algorithm

Case	Training accuracy	Testing accuracy
Mass Removal (SVM+ PI)	97.45	97.91
Mass Removal (SVM+PCA)	98.41	96.57
Mass Addition (SVM+PI)	92.8	91.57
Mass Addition (SVM+PCA)	98.21	93.45

Logistic regression results for mass addition of 23.5 grams between sensors 103 and 104

Sensor Trial	X – 103	Y – 103	Z – 103	X – 104	Y – 104	Z – 104
1	0.743	0.707	0.768	0.681	0.427	0.670
2	0.948	0.917	0.893	0.544	0.988	0.517
3	0.987	0.94	0.974	0.968	0.953	0.717
4	0.687	0.675	0.714	0.546	0.755	0.994
5	0.841	0.931	0.785	0.998	0.984	0.814
6	0.952	0.889	0.785	0.702	0.791	0.576
7	0.994	0.987	0.983	0.981	0.995	0.798
8	0.996	0.986	0.781	0.944	0.929	1
9	0.576	0.595	0.511	0.799	0.606	0.8066
10	0.945	0.766	0.852	0.778	0.586	0.854

Accomplishments – Smart Film

- Milestone: Demonstrate Smart Layer in Representative Piping Structural Component
- Methods: 1) Grow smart film from carbon steel surface OR

  2) Grow smart film from non-corroding surface and affix near carbon steel surface.

Method 1

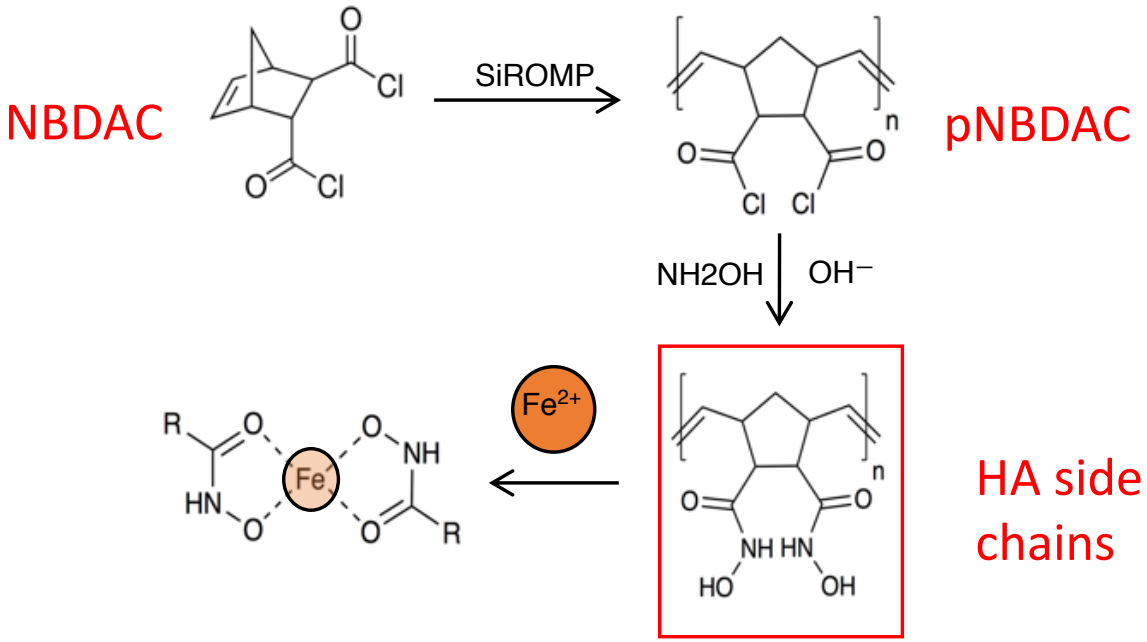

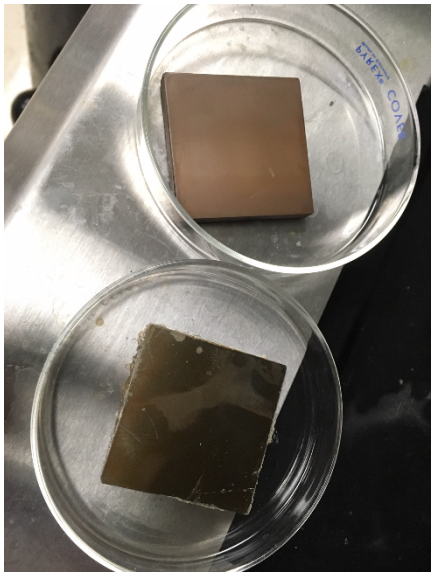

Accomplishments – Smart Film

- Method 2: Grow smart film from non-corroding surfaces

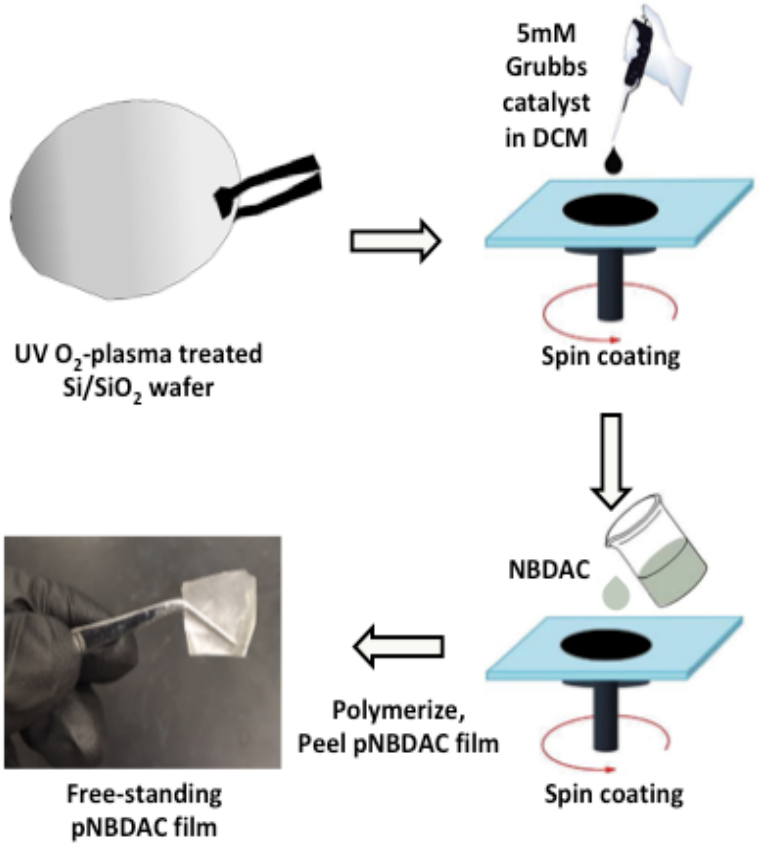

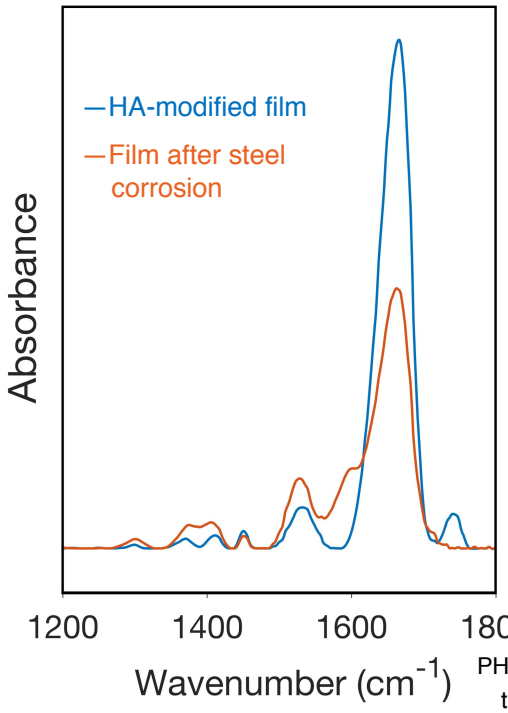

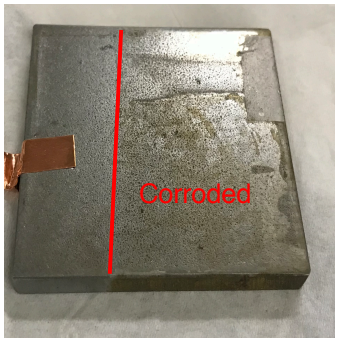

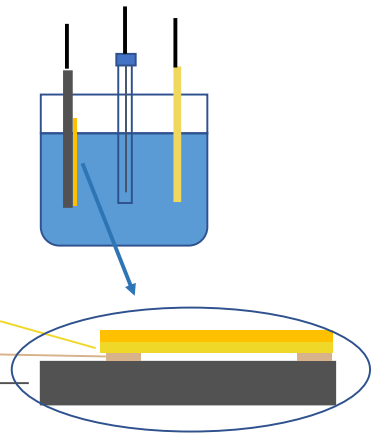

Expand growth of film to silicon and achieve thicker, free-standing films.

Smart film captures metal ions due to corrosion of a nearby carbon steel surface.

Accomplishments – Sensing Metal Chelation

- Vibroacoustic detection of the smart film and chelation

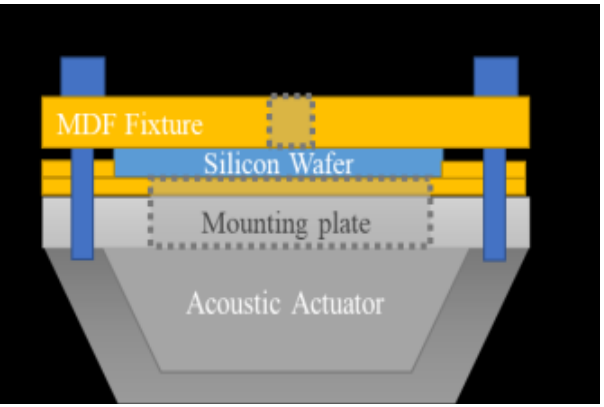

Schematic of test fixture design.

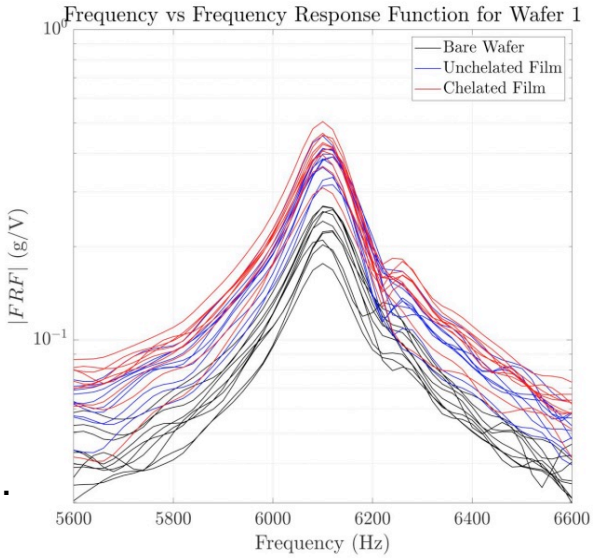

Frequency response function for Wafer 1, illustrating a trend between stage of film and peak amplitude.

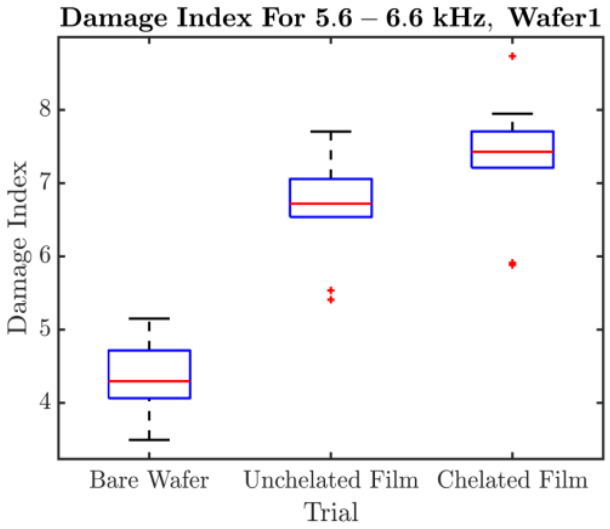

Damage indices for each stage of chelation.

Accomplishments – Mapping of Internal Damage

- Objective: Map Internal Damage in a Piping Structural Component using Measurements on the Outside of Pipe.

- Method: Analyze effects of changes on inner surface of metal surface on the vibro-acoustic response of external surface.
  - Uneven mass loss changes the coupling between bending and torsional vibration that can be sensed.
  - The transmissibility function between the vertical bending (z) and torsional motion (θ) for the ith accelerometer was calculated:

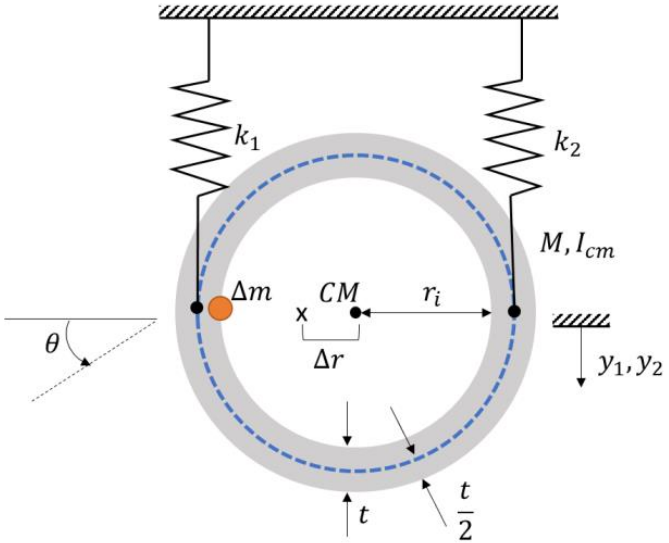

$$T(\omega)_{z_i \to \theta_i} = \frac{G_{xx,\theta}(\omega)_i}{G_{xx,z}(\omega)_i}$$

Accomplishments – Mapping of Internal Damage

- The pipe elbow fitting was instrumented with 6 triaxial accelerometers, arranged within a global coordinate system, was installed in the pipe circuit testbed.
- Mass was evenly removed from the inside diameter of the elbow (see gold shaded area) in percent increments of mass relative to the total initial mass of the pipe elbow.
  - The undamaged pipe: 6350 g
- Logarithm of relative transmissibility magnitude was calculated in a contour plot for each mass removal to illustrate the mass change results.

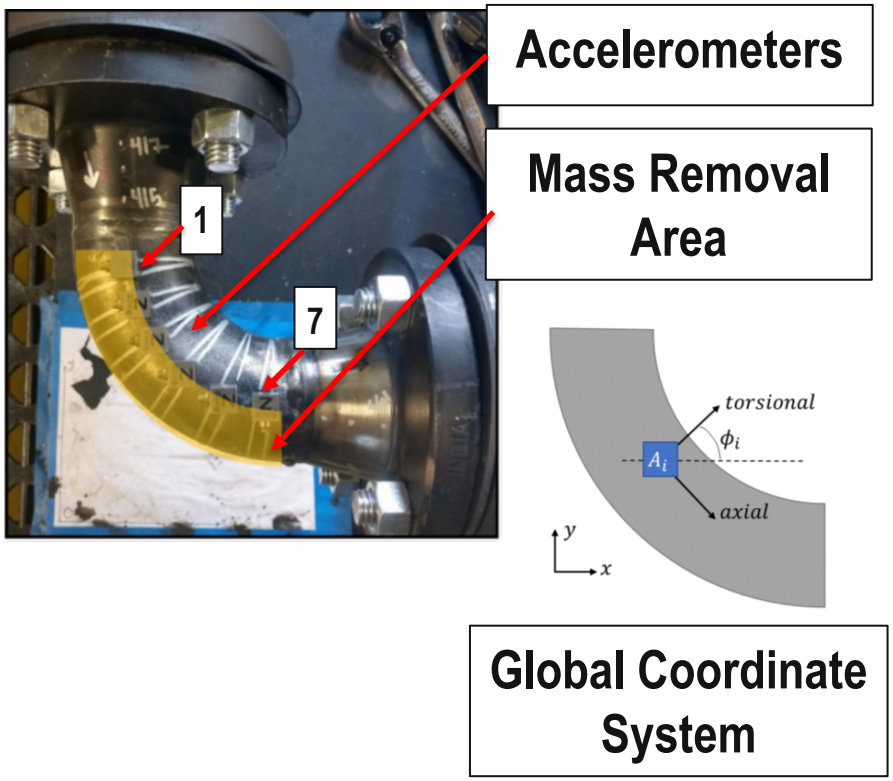

$$T_{z\to\theta}(\omega)_r = \log\left(\left|\frac{T_{z\to\theta}(\omega)}{T_{z\to\theta}(\omega)'}\right|\right)$$

Note: For unchanged transmissibility, the relative transmissibility equation goes to zero

Accomplishments – Mapping of Internal Damage

- The relative transmissibility contours across successive pairs of 6 accelerometers are shown for the undamaged pipe and for 0.3% and 1.0% mass reduction, respectively
- Results: The relative transmissibility shift between the bending and torsional degrees of freedom observed at accelerometers 4 and 5, located over the damaged area, exhibited a steady increase due to the imbalance caused by the mass loss.

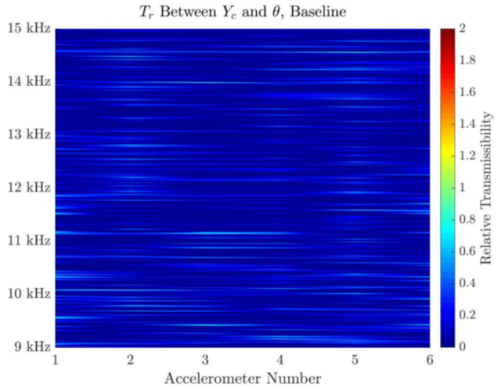

Baseline (undamaged) pipe elbow

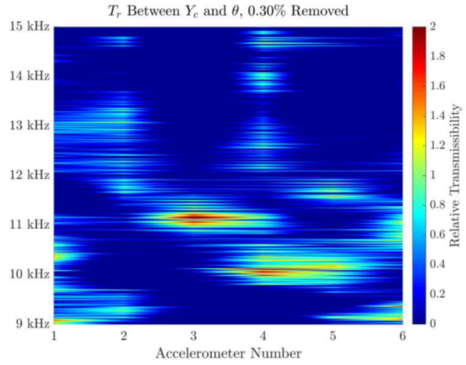

0.3 % mass removes from the pipe elbow

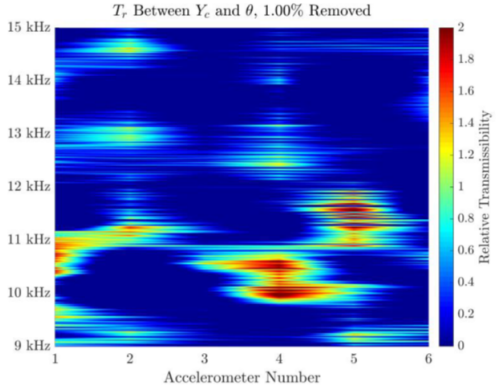

1.0 % mass removes from the pipe elbow

Accomplishments – Power Harvesting

- Objective: Demonstrate Thermoelectric Power Harvesters
- Method: Developed a 3D conformal aerosol jet printing method to fabricate flexible thermoelectric (TE) devices for power harvesting. The printed TE films show peak TE power factor of 2.2 mW/m·K^2.

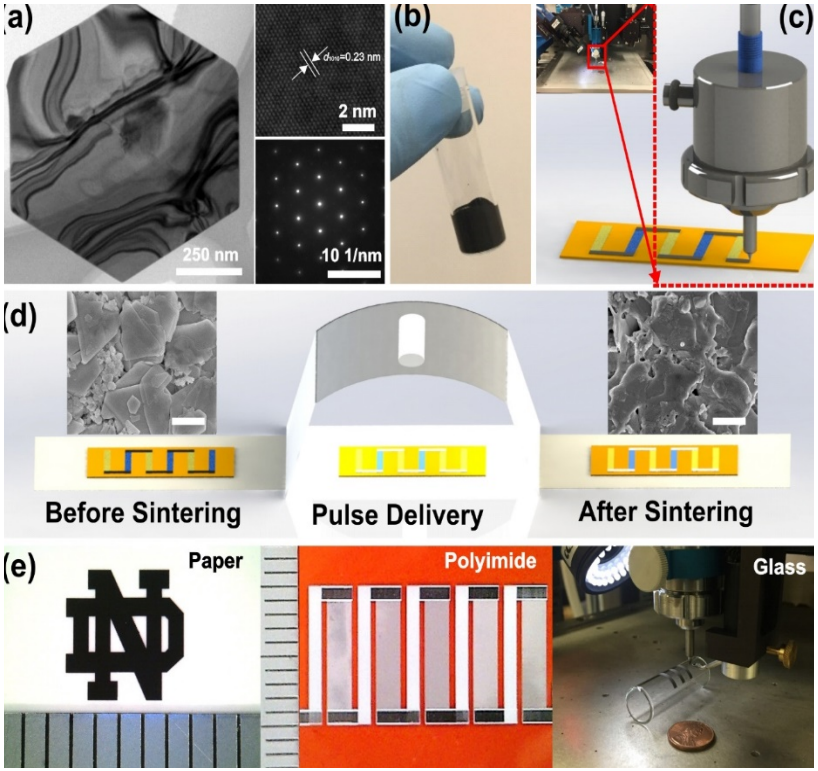

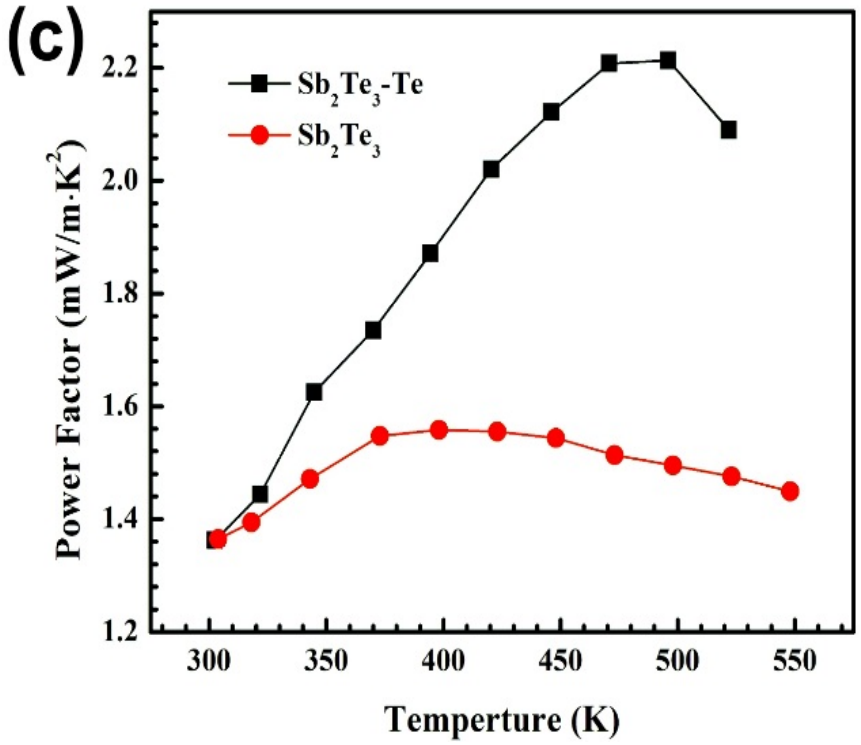

M. Saeidijavash, **Y. Zhang* et.al.**, ***Advanced Functional Materials***, 1901930, 2019
C. Dun, **Y. Zhang* et.al.**, ***Advanced Science***, in press, 2019

Accomplishments – Power Harvesting

Key Results:

- Demonstrated aerosol jet printed (AJP) flexible thermoelectric generator:
  - produces a maximum electrical power density of about 8 mW/cm^2 with a temperature gradient of 60 K
  - can be printed on curves surfaces with a very high spatial resolution about 10 um in line width
- Developed novel TE inks that are printable using the AJP method

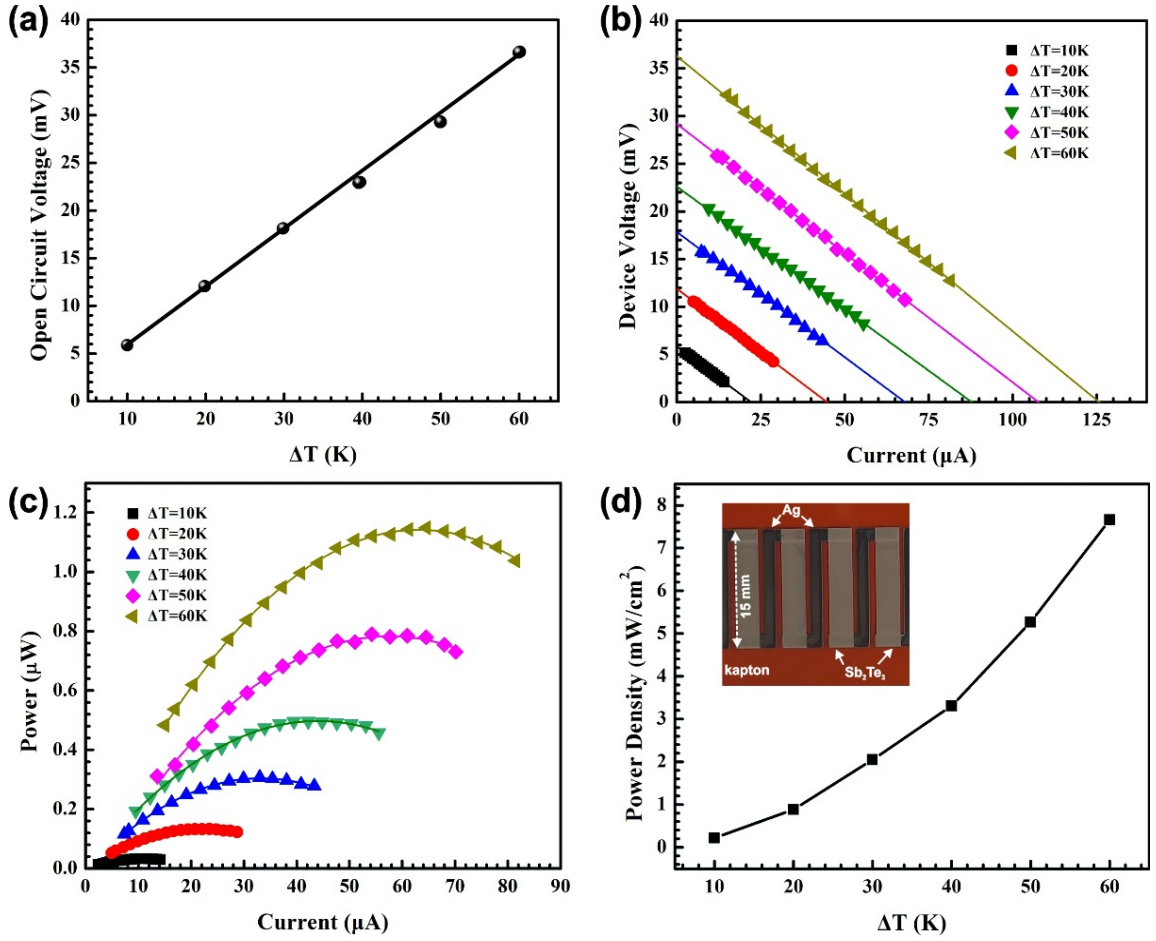

(Note: The thermoelectric generator (TEG) printed last year was based on screen printing, which can only print devices on flat surfaces, that produces higher power density (approximately 15 mW/cm^2) mainly because it uses very viscous TE paste)

Technology Impact (1)

Describe how this technology:

- *Advances the state of the art for nuclear application*
  - A suite of smart sensors and diagnostic algorithms to provide **a solution for monitoring and 3D mapping of damage in critical piping areas**.
    - E.g., smart film on the inner wall of the pipe could do something that is impossible today, that is, the film could detect earliest stage corrosion.
- *Supports the DOE-NE research mission*
  - Continuously certify that nuclear power plants are safe to operate with monitoring as an **economically efficient approach**.
    - Corrosion is very difficult to detect especially in the early stages.
    - Approx. 70 miles of piping in nuclear power plants to inspect.
    - Inspections turn up no damage 99% of the time.
  - Students who are being trained in this project are being exposed to an area of national need.

Technology Impact (2)

Describe how this technology:

- *Impacts the nuclear industry*
  - This kind of health monitoring system for the pipes used in a cooling circuit system for a nuclear power plant can help **to reduce inspection/maintenance costs** and outages saving consumers money.

Courtesy: http://www.nbcnews.com/

- *Will be commercialized*
  - Monitoring of much of the cooling circuit can be addressed using guided wave technology so we are focusing on the joints and the regions of the pipe downstream of the joint such as the elbows and T sections to address commercial need.
  - **This strategy is scalable to facilitate commercialization** because it focuses on the optimization and implementation of the 3D sensor network to specific regions of interest in a large circuit.

Publications

Year 2018:

- Vanderbilt University:
  - X. Deng and G. K. Jennings, “Surface-Initiated Polymerization of trans-5-Norbornene-2,3-Dicarbonyl Chloride: A Versatile Platform for Tailored Polymer Film Compositions,” 2018, Langmuir (Jennings)

Year 2019:

- Vanderbilt University:
  - X. Deng, L. Prozorovska, and G. K. Jennings “Metal Chelating Polymer Thin Films by Surface-Initiated ROMP and Modification,” J. Phys. Chem. C, 2019, 123, 23511-23519. (Jennings)
  - X. Deng, J. L. Livingston, N. J. Spear, and G. K. Jennings "pH-Responsive Copolymer Films Prepared by Surface-Initiated Polymerization and Simple Modification," Langmuir, 2019, submitted. (Jennings)
  - Brubaker C., Newcome, Kailey, Jennings, Kane, Adams, Douglas. “3D-Printed Alternating Current Electroluminescent Devices.” 2019, Journal of Materials Chemistry C, DOI: 10.1039/C9TC00619B (Adams and Jennings)
- University of Notre Dame:
  - C. Dun, W. Kuang, N. Kempf, M. Saeidi-Javash, D. Singh, and Y. Zhang, 3D Printing of Solution-Processable 2D Nanoplates and 1D Nanorods for Flexible Thermoelectrics with Ultrahigh Power Factor at Low-Medium Temperatures, Advanced Science, 1901788, 2019. (Zhang)
  - M. Saeidijavash, W. Kuang, C. Dun, and Y. Zhang*, Three-Dimensional Conformal Printing and Photonic Sintering of High-Performance Flexible Thermoelectric Films Using 2D Nanoplates, Advanced Functional Materials, 1901930, 2019 (Zhang)

Conclusions

Diagnostic algorithms showed promising results and will be enhance in third year to support prognosis.

Smart film thickness and area can be scaled up by new spin coating approach, and corrosion products are captured in nearby carbon steel surface.

Vibroacoustic methods show different frequency responses for bare wafer versus film-coated versus iron-chelated film.

Damage mapping of material loss in pipes was achieved using array of multi-axis accelerometers to detect coupling of modes.

Printed flexible thermoelectric generator that produces a maximum power density of 8 mW/cm$^{2.}$

Questions

- *douglas.adams@anderbilt.edu any additional questions that may not be answered during the webinar.*

Clean. **Reliable. Nuclear.**